

An exhaustive non-linear modelling of GaInP/GaAs HBT's Application to a low phase noise Ku Band VCO

R.Plana¹, T.Parra¹, C.Zanchi¹, J.M.Dienot¹, M.Gayral¹, M.J.Villard², J.C.Martin², P.G. Tizien³ and J.Graffeuil²

¹ LAAS-CNRS & Université Paul Sabatier Toulouse 7 Av du Colonel Roche 31077 Toulouse Cedex, France

² DASSAULT Electronique 55, quai Marcel Dassault, BP 301, 92214 St Cloud Cedex, France

³ CNES Toulouse 18 Av Edouard Belin 31055 Toulouse France

Abstract

This paper presents an exhaustive non-linear modelling including the low-frequency noise sources which has been implemented to design a low-phase noise voltage controlled oscillator in the Ku band with a 1 GHz bandwidth and a -92 dBc/Hz at 100 kHz carrier offset phase noise level.

Introduction

Heterojunction bipolar transistors (HBT's) based on the GaInP/GaAs material system have received considerable interest as a replacement for AlGaAs/GaAs HBT's since they have shown superior performance in terms of microwave [1,2] and noise properties [3,4,5].

In this paper, we present the design of a low phase noise Ku band VCO using a commercial microwave simulator, based on a complete non-linear modelling of GaInP/GaAs HBT's including noise sources.

Section I is dedicated to a presentation of the HBT samples which are involved in this work. Section II deals with DC and pulsed characterisation. Section III addresses S parameter measurements in order to extract a small signal equivalent circuit. Section IV presents low-frequency noise measurements and modelling which have been carried out on HBT's samples. Section V addresses the non-linear model presentation and its validation. Finally in section VI, we present the design and the performances of the hybrid Ku band VCO.

I-Device characterisation

The microwave HBT devices were fabricated on MOCVD grown GaInP/GaAs structures on SI GaAs substrate using a fully self-aligned process by LCR Thomson. The key elements are essentially : a highly C doped base to ensure a low p dopant diffusion into emitter which minimise the recombination, an extremely selective emitter etching. An appropriate passivation has been used to reduce the surface recombination. This technology yields excellent RF performance with cut-off frequency (f_t) and maximum oscillation frequency (f_{max}) in the 40 GHz range for a two $2 \times 30 \mu\text{m}^2$ emitter fingers HBT.

The large signal model topology is based on Ebers-Moll one and include the noise sources. It involves four non-linearities (E-B and C-B junctions, output current source and E-B capacitance) plus two input noise generators which are described by non-linear equations versus frequency and bias. We are going now describe the used procedure to establish it.

II-DC an pulsed characterisation

Current voltage characteristics, static current gain (β) plots, forward and reverse Gummel plots and breakdown voltage determination realise the first steps for assessing the model in order to determine some functional parameters like the offset voltage, the ideality factors of Emitter-Base and Collector-Base junctions and their corresponding saturation current values. DC characterisation provides a first estimation of the resistive parts of the device (Collector, Base and Emitter resistances). To take into account HBT self thermal effects, additional pulsed output current-voltage characteristics $I_{ce}=f(V_{ce}, I_b)$ measurements are performed with a DC quiescent point corresponding to the device biasing in the oscillator (A class operation) : $V_{ce}=4$ V and $I_c=17$ mA.

III S- Parameter and Capacitances Measurements

Then, S-parameter measurements were performed from 100 MHz up to 40 GHz for the chosen DC bias point on four different devices. From this measurements, cut-off (f_t) and maximum oscillation (f_{max}) frequencies are obtained and the results which are summarised in table 1 indicate that all the values are regrouped around 40 GHz which is an indicator of the good maturity of this technology.

Device	f_t (GHz)	f_{max} (GHz)
#1	33.2	37
#2	40	37.4
#3	33.2	38.6
#4	35.6	38.6

Table 1 :

On fig.1 we have reported the small signal equivalent circuit topology which is implemented in MDS software to compute the scattering parameters from 100 MHz to 40 GHz.

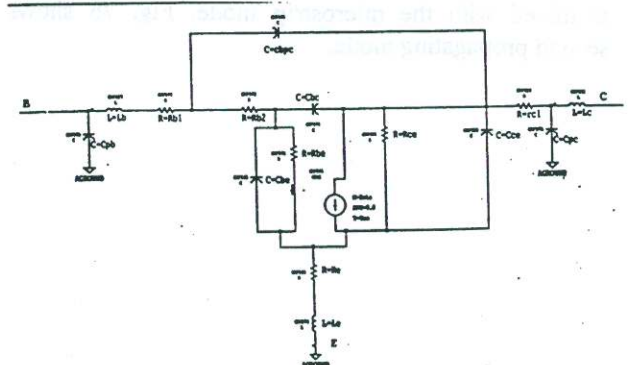


Fig.1: small signal equivalent circuit topology

On fig 2a and 2b, we have plotted the measured and modelled data for device #1 which indicate an excellent agreement between measured and calculated values. The small signal parameters are summarise in table 2.

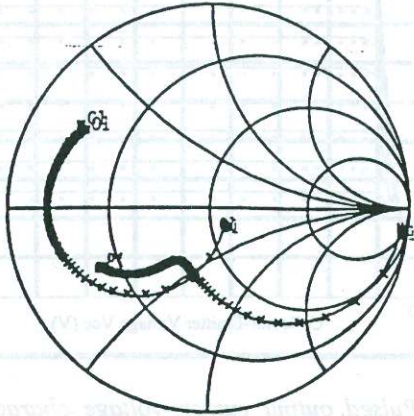


Fig 2.a : S11 and S22 parameters from 100 MHz to 40 GHz

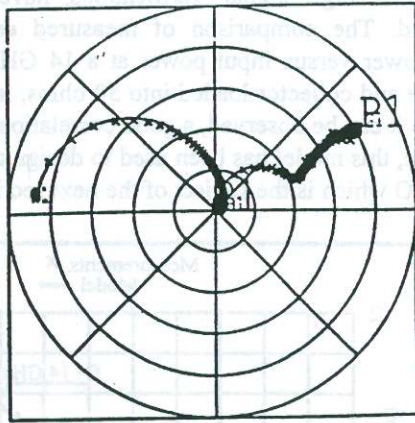


Fig 2.b : S21 and S12 parameters from 100 MHz to 40 GHz

Extrinsic parameters		Intrinsic parameters	
Lc(pH)	13.8	Cbc(fF)	30.7
Lb(pH)	45.5	Cbe(pF)	2.17
Le(pH)	11	Rb2(Ω)	4.1
Cpb(fF)	28.6	Rce(Ω)	3020
Cpc(fF)	0.1	Rbe(Ω)	52
Cbpc(fF)	146.9	β	17.5
Cce(fF)	62.5	τ(ps)	2.2
Rc1(Ω)	2.46		
Re(Ω)	0.1		
Rb1(Ω)	1.34		

Table 2

The characterisation of E-B and C-B capacitances were performed at a 10 MHz frequency versus bias in order to determine their voltage dependence by non-linear equations. The next section is dedicated to the low-frequency (L.F) noise measurements.

III L.F Noise Measurements

A full low-frequency noise characterisation of HBT is obtained by measuring the input noise voltage and input noise current generator including their correlation from 250 Hz to 100 kHz. This is achieved by using a multiple impedance multiple [6] and an appropriate numerical

procedure [7]. L.F noise measurements have been carried out from base bias current ranging from 75 μA to 1 mA at Vce=4 V. The noise spectra (see fig 3a and 3b) result from the superposition of white noise, 1/f noise and a generation-recombination (g-r) noise components (related to a discrete trap in the extrinsic base region). The input noise generators can be expressed as follows :

$$i_n^{-2} = 2qIb + \frac{2qIc}{\beta^2} + \frac{A_i}{f} + \frac{C_{i1}/f_{i1}}{1 + (\frac{f}{f_{i1}})^2} \quad (1)$$

$$e_n^{-2} = 4kTr'_b + r_b'^2 2qIb + \frac{2qIc}{\beta^2} (r'_b + r_{be})^2 + \frac{A_v}{f} + \frac{C_{v1}/f_{v1}}{1 + (\frac{f}{f_{v1}})^2} \quad (2)$$

Where $r'_b = r_{b1} + r_{b2} + r_e$ $r_{be} = \frac{U_t}{I_b}$ $\beta = \frac{I_c}{I_b}$

A_i , A_v are respectively the 1/f amplitude of noise current and noise voltage generators. C_{i1} , C_{v1} represent respectively the g-r noise component amplitude of noise current and noise voltage generators and f_{i1} , f_{v1} are related to a time constant of trapping-detrapping process respectively involved in noise current and noise voltage spectra.

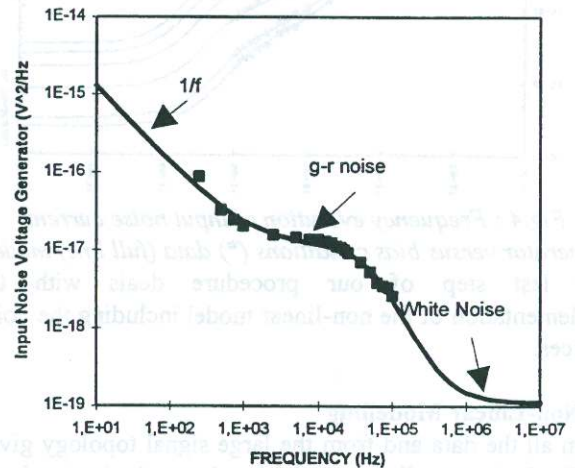


Fig 3a : frequency evolution of input noise voltage generator (■) data (full line) model for base bias point fixed at $I_b=250 \mu A$, and $V_{ce}=4 V$

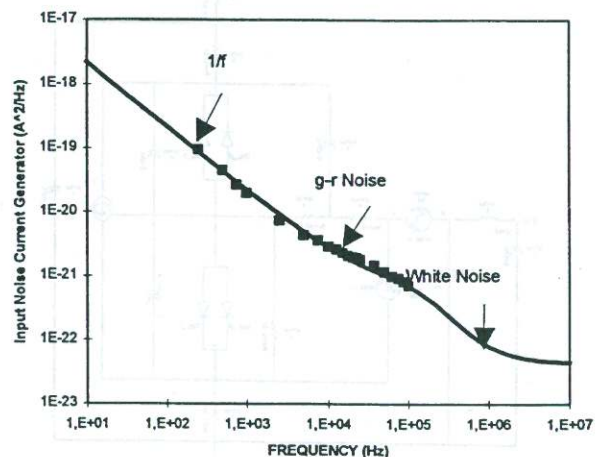


Fig 3.b: frequency evolution of input noise current generator (■) data (full line) model for base bias point fixed at $I_b=250 \mu A$, and $V_{ce}=4 V$

Finally a full description of L.F noise behaviour versus bias conditions is given by the following expressions.

$$i_n^{-2} = 2qI_b + \frac{2qI_c}{\beta^2} + \frac{A_i I_b^{\alpha 1}}{f} + \frac{B_i I_b^{\alpha 2}}{1 + \left(\frac{f}{f_o I_b^{\alpha 3}}\right)^2} \quad (3)$$

$$e_n^{-2} = 4kT r_b' + r_b'^2 2qI_b + \frac{2qI_c}{\beta^2} (r_b' + r_{be})^2 + \frac{A_v I_b^{\beta 1}}{f} + \frac{B_v I_b^{\beta 2}}{1 + \left(\frac{f}{f_o I_b^{\beta 3}}\right)^2} \quad (4)$$

We have reported in fig.4 the frequency evolution of the input noise current generator versus bias conditions and we note an excellent agreement between the measured and predicted noise levels.

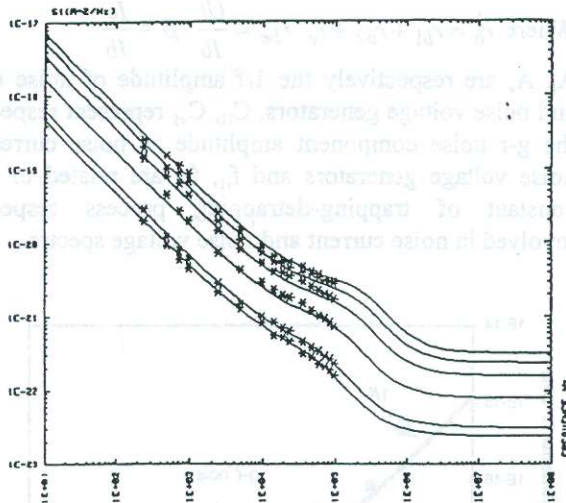


Fig.4 : Frequency evolution of input noise current generator versus bias conditions (*) data (full line) model. The last step of our procedure deals with the implementation of the non-linear model including the noise sources.

IV Non-Linear Modelling

From all the data and from the large signal topology given on Fig.5, the non linear model has been obtained using a microwave commercial software (HP MDS) by fitting both the pulsed output current voltage characteristics (see fig.6) and the forward Gummel plots.

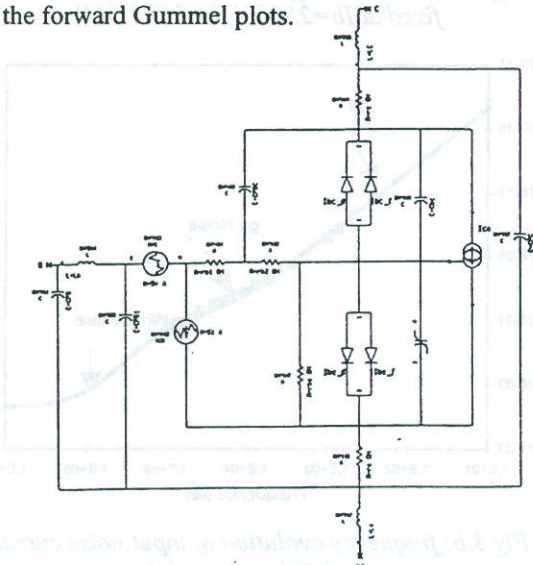


Fig.5 : Large signal model topology

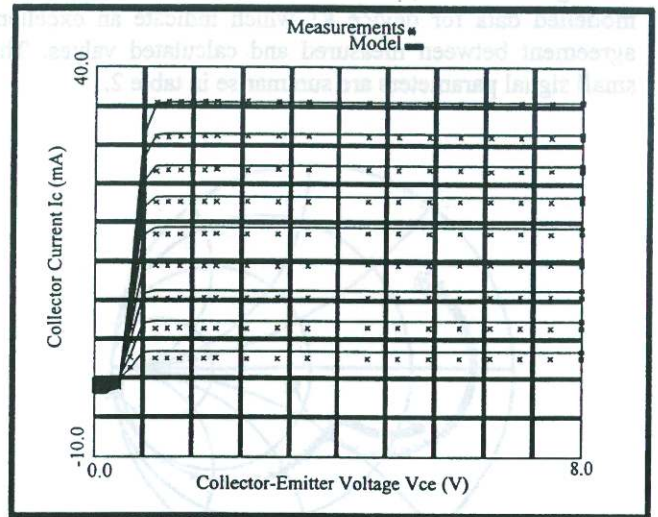


Fig.6 : Pulsed output current-voltage characteristics (*) measured and (full line) modelled for a quiescent point fixed at $I_c=17 \text{ mA}$ and $V_{ce}=4 \text{ V}$

Small and large signal verifications have then been performed. The comparison of measured and predicted output power versus input power at a 14 GHz frequency, with base and collector loaded into 50 ohms, is reported on Fig.7. As it can be observed, a good correlation is obtained. Therefore, this model has been used to design an hybrid Ku band VCO which is the subject of the next section.

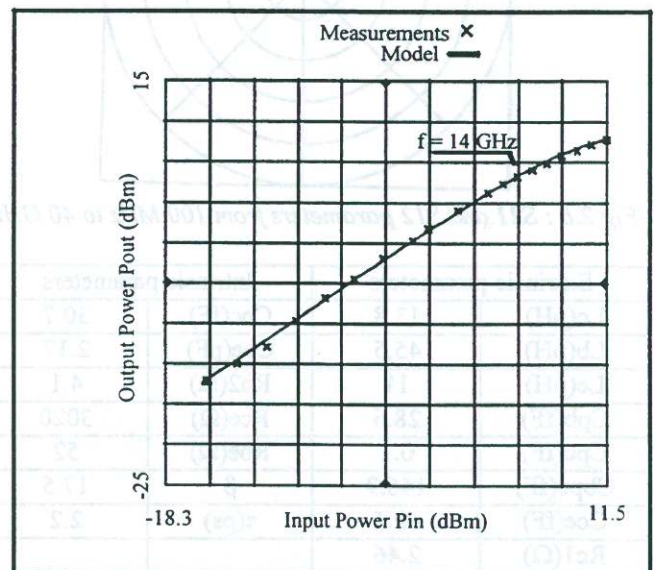


Fig.7. : Output power versus input power at 14 GHz with input and output 50 Ohms loaded

IV-Design and test of the VCO

The VCO topology was optimised in order to minimise the phase noise level and to obtain a 1 GHz bandwidth in the Ku frequency band. This optimisation led to the implementation of a common emitter oscillator with a serial feedback in the emitter, a varactor on the HBT base terminal and a LC series resonator on the collector.

We have reported on Fig.8 the equivalent circuit of this oscillator.

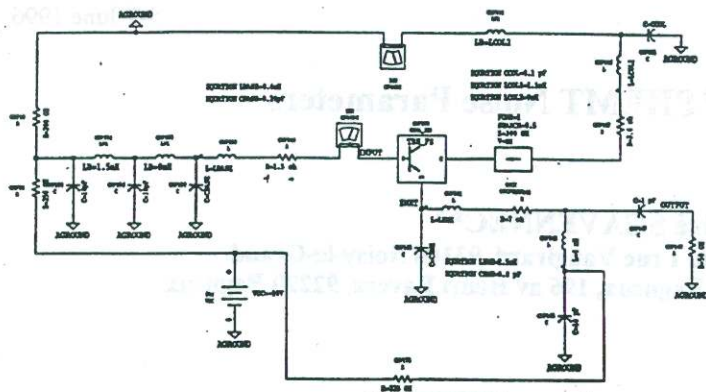


Fig.8 : Equivalent circuit topology of the VCO

Owing to the observed HBT LF noise, phase noise in the range of -95 dBc/Hz at 100 kHz offset is predicted with electrical simulations.

The VCO has been realised in hybrid technology on an alumina substrate. This circuit exhibits measured performances in good agreement with predicted ones. Phase noise levels ranging from -90 dBc/Hz to -92 dBc/Hz have been actually measured at 100 kHz carrier offset. In order to compare this result with other published we have performed a comparative study of phase noise of HBT oscillator. To facilitate the comparison phase noise have been normalised with respect to carrier frequency f_c (14.3 GHz) and with respect to offset frequency f_b (100 kHz). Expected phase noise is obtained assuming a $1/f_c^2$ and $1/f_b^3$ dependences and the results are plotted on Fig.9.

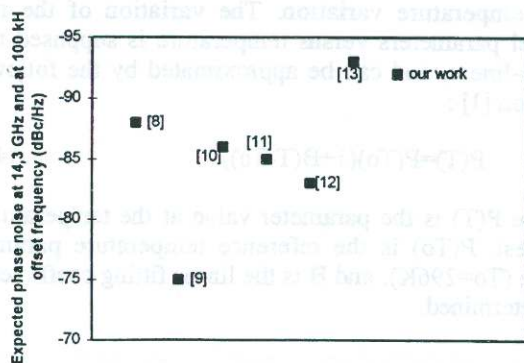


Fig.9 : Comparative study of phase noise performance of some micro-wave solid state oscillators

The results indicate that our work is among the best results never recorded in terms of phase noise level. Finally, we have performed phase noise measurements versus temperature ranging from 230K to 350 K and the results indicate that we note an improvement of the phase noise level at 100 kHz offset frequency and this behavior is correlated with the variations of both the input noise voltage and input noise current generators at this frequency. There is a decrease of noise due to a shift of the g-r noise component.

Conclusion

A complete non-linear modelling of GaInP/GaAs HBT's including LF noise sources is presented. This model has been used for the design of a low phase noise Ku-band VCO. The measured performances (frequency tuning range of 1 GHz associated with a phase noise level of -92 dBc/Hz at 100 kHz carrier offset) compare very well with predicted

ones. A comparative study indicate us that the observed phase noise is among the best ever obtained on a Ku-band VCO.

References :

- [1] H.Leier et al « High speed self-aligned GaInP/GaAs HBT's » Electronics Letters, vol 29, n°10 pp 868-870, 1993.
- [2] W.Liu et al « Microwave performance of self-aligned GaInP/GaAs heterojunction bipolar transistor » IEEE Trans on ED, vol 14, pp 176-178, 1993.
- [3] M.T.Fresina et al « high speed, low-noise InGaP/GaAs Heterojunction bipolar transistor » IEEE EDL, vol 16, n°12, pp 540-541, Dec 1995.
- [4] W.J.Ho et al « GaInP/GaAs HBT's for high-speed integrated circuits applications » IEEE EDL, vol 14, n°12, pp 572-574, Dec 1993.
- [5] R.Plana et al « Low-frequency noise in self-aligned GaInP/GaAs heterojunction bipolar transistors » Electronics Letters, vol 28, n°25, pp 2354-2355, Dec1992.
- [6] J.Graffeuil and R.Plana "Low-frequency noise properties of microwave transistors and its application to circuit design" Invited paper at 24th European Microwave Conference Cannes 1994, pp1-13.
- [7] L.Escotte, R.Plana and J.Graffeuil "Evaluation of noise parameters extraction methods" IEEE Trans on MTT, Vol41, N°3,, March 1993, pp 382-387.
- [8] U.güttich et al "Ka-Band monolithic VCOs for low noise applications using GaInP/GaAs HBTs" IEEE MTT-S, 1994, pp 131-134.
- [9] H.Blanc et al " Fully Monolithic Ku and Ka Band GaInP/GaAs HBT wideband VCOs" IEEE MTT-S, 1994, pp 127-130.
- [10] Madhian and Takahashi "a low-noise K-Ka Band oscillator using AlGaAs/GaAs heterojunction bipolar transistors" IEEE Trans on MTT, vol 39, n°1, pp 133-136, 1991.
- [11] Yamauchi Y, H. Kamitsuna, M. Nakatsugana, H.Ito, M.Muraguchi and K.Osafune "A 15 Ghz monolithic low-phase noise VCO using AlGaAs/GaAs HBT technology" IEEE J of Solid State Circuits, vol 27, n°10, pp 1444-1447,1992.
- [12] J.Cowles, L.Tran, T.Block, D.Streit, C.Grossman, G.Chao and A.Oki "A comparison of low-frequency noise in GaAs and InP based HBTs and VCOs" IEEE MTT-S, 1995, pp 689-692.
- [13] H.Wang, K.W.Chang, L.Tran, J.Cowles, T.Block, D.C.W Lo, G.S Dow, A.Oki, D.Streit and B.R Allen "Low phase noise millimeter-wave frequency sources using InP based HBT technology" IEEE GaAs IC symposium 1995, pp 1-4.